2024 IEEE/ASME International Conference on Advanced Intelligent Mechatronics (AIM)
July 15-19, 2024. Boston, MA, USA

Adaptive Movement Tracking for Prostate Organ in Robot-Assisted Brachytherapy Treatment

Abdeslem Smahi, Othman Lakhal, Mario Sanz Lopez, David Pasquier and Rochdi Merzouki

***Abstract*—This manuscript presents a sophisticated robotic system that incorporates an adaptive optimization algorithm specifically designed for brachytherapy in the treatment of prostate cancer. The central innovation of this system lies in the algorithm itself, which is crafted to dynamically alter needle paths based on the real-time movements of the prostate gland during the local procedure. The algorithm utilizes real-time positional information derived from Magnetic Resonance Imaging (MRI) to guarantee precise localization of the prostate, adapting to its continual motion and deformation. This level of accuracy is of paramount importance in brachytherapy, as the precise positioning of radioactive seeds directly influences the effectiveness of the therapy and reduces harm to nearby healthy tissues.**

Our findings demonstrate a noticeable enhancement in the precision of radiation seed placement, leading to a more efficient delivery of radiation. Additionally, the adaptive characteristics of the algorithm notably decrease the frequency of needle insertions, resulting in a less invasive treatment process for patients. This reduction in the number of needle insertions also contributes to a reduction in the risk of infection and a shorter recovery period. This innovative robotic system, which is complemented by the adaptive optimisation algorithm, enhances the coverage of targeted areas achieved through a conventional combinatorial approach by approximately 12% while requiring fewer needles.

***Index Terms*—Medical robot, Adaptive Optimisation, Prediction, Path planning, Magnetic resonance imaging**

I. Introduction

Prostate cancer, the most common malignancy in men, generally requires treatments such as surgery, external radiotherapy, or brachytherapy (BT), all of which are approved by the High Authorities for Health (HAH). These treatments are implemented through a multidisciplinary approach involving urologists and radiation oncologists, with the patient making the ultimate decision. Surgery involves removing the entire prostate, whereas external radiotherapy delivers a dose of 70Gy ($Gray$) across 35 sessions using a particle accelerator. Brachytherapy, which is less invasive for the patient, aims to irradiate the target area with either low-dose (LDR) or high-dose (HDR) ionizing radiation, typically guided by transrectal ultrasound (TRUS). Known as TRUS-BT, this method has been the standard for directing brachytherapy procedures. However, several inherent issues arise with this technique, the rigid grid used in TRUS-BT restricts insertion angles, and prostate movement during the procedure can cause incorrect seed placement [1]. Additionally, TRUS may not clearly distinguish cancerous tissue, impacting the precision of seed placement [2].

To mitigate these limitations, robotic systems have been developed, including those that replicate manual procedures and grid-free robots that provide increased flexibility and accuracy in seed placement [2], [3]. The needle insertion process in brachytherapy or biopsy [4] is vital for the success of the treatment and the patient's overall experience. Key objectives for optimizing this procedure include reducing surgery time, minimizing needle adjustments, improving seed placement accuracy, decreasing radiation exposure, and enhancing patient comfort.

Given these considerations, in this paper:

- We present a novel algorithmic approach that enhances the robot's efficiency in MRI-guided prostate.
- We provide a comprehensive comparison of our approach with existing methodologies, highlighting its performance in terms of accuracy and efficiency.
- Through extensive simulations and real-world tests, we demonstrate the practical applicability and benefits of our approach.

II. MR-robot for Prostate intervention

The CoBra robot is a 5-DoF parallel robot for minimally invasive procedures. It uses five linear actuators powered by MRI-compatible piezo-sonic motors with high precision. Absolute encoders ensure reliable position control, critical for preventing procedure interruptions due to power failures. The robot operates within a 3T MRI scanner, guiding needles transperineally while providing real-time visualization through an MR-safe camera, as depicted in Fig. 3. This setup allows for optimal oblique needle insertions, reducing patient trauma and improving procedural efficiency.

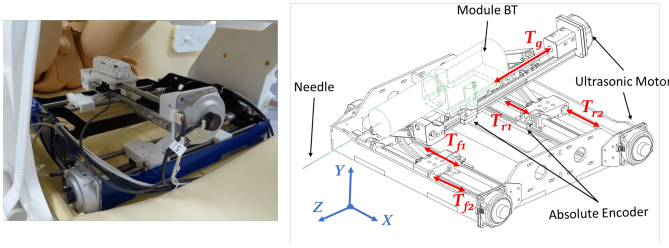

Fig. 2. Overview of the CoBra 5-DoF Parallel Robot

III. CoBra Robot Kinematics

This section develop the CoBra robot Inverse Kinematic Model (IKM), is a nonlinear function f_{IKM}, allowing to describe the position of the finite target points (needle tip or

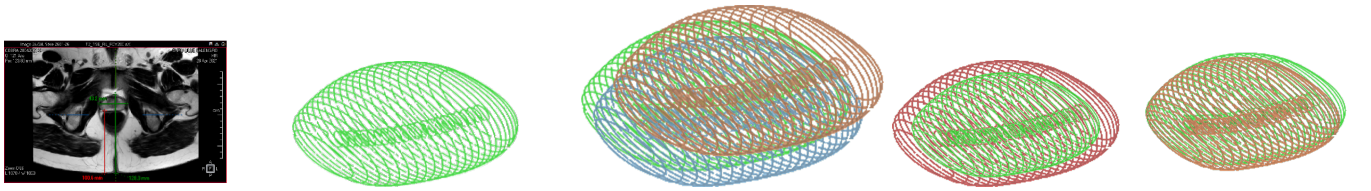

(a) MR image of the Prostate organ taken in lithotomy position

(b) Prostate 3D model

(c) Illustration of Prostate movements (each color is a new position)

(d) Illustration of Prostate Inflammation

(e) Illustration of Prostate deformation

Fig. 1. Prostate Motions and Movements Illustrations

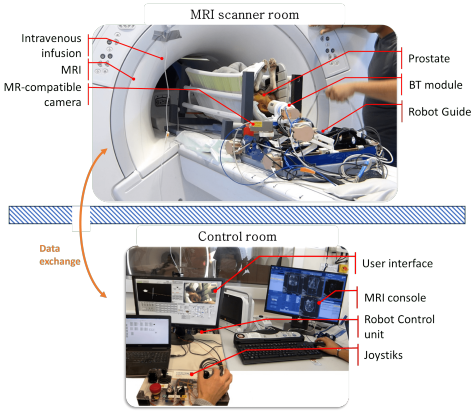

Fig. 3. The CoBra system includes a 5-DoF parallel robot for needle guidance, a BT module, an MRI scanner, and an MR camera. The sedated patient (an animal) is positioned in lithotomy. The system allows tele-operation via a joystick from the control room, using the MRI console and a graphical interface.

Tool Centre Point - TCP) (x_t, y_t, z_t) to the 5 joint positions of the robot $(L_{f_1}, L_{f_2}, L_{r_1}, L_{r_2}, L_g)$, as follows:

$$[L_{f1}, L_{f2}, L_{r1}, L_{r2}, L_g] = f_{IKM}(x_t, y_t, z_t) \tag{1}$$

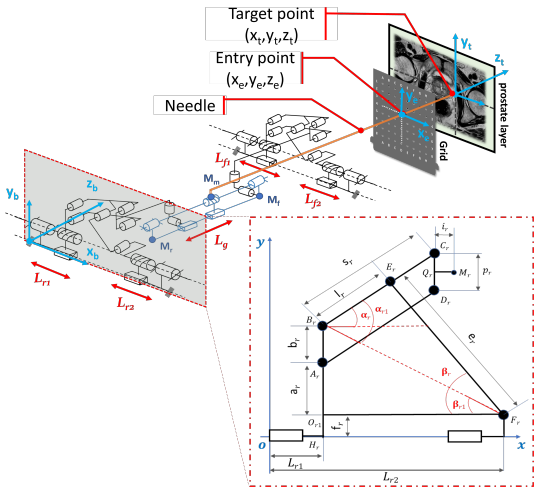

Fig. 4. CoBra Robot kinematics

The target point can be reached with various needle orientations. The input grid prevents needle bending but limits the needle's movement, reducing possible paths to the target. The kinematic model must control the needle tip and verify its accessibility within these constraints.

Let a target point be defined by the transformation matrix ${}^t_bT$ expressed in the base frame $\Re_b\{x_b, y_b, z_b\}$ of the robot (Fig. 4).

$${}^t_bT = \begin{bmatrix} u_1 & v_1 & w_1 & x_t \\ u_2 & v_2 & w_2 & y_t \\ u_3 & v_3 & w_3 & z_t \\ 0 & 0 & 0 & 1 \end{bmatrix} \tag{2}$$

Knowing the desired entry point and target point, it is therefore possible to determine the directional vectors. $\mathbf{u}, \mathbf{v}$ and $\mathbf{w}$ of the reference frame attached to the point M_f along the direction M_rM_f. Based on the coordinates of the entry point $\{x_e, y_e, z_e\}$ and the target point $\{x_t, y_t, z_t\}$, the vector $\mathbf{w}$ can be obtained as follows:

$$\mathbf{w} = \frac{[x_t - x_e \ , \ y_t - y_e \ , \ z_t - z_e]^T}{\sqrt{(x_t - x_e)^2 + (y_t - y_e)^2 + (z_t - z_e)^2}} \tag{3}$$

The vector $\mathbf{u}$ is normal to the vector $\mathbf{w}$ and is parallel to the plane ZX

$$\mathbf{u} = \frac{[w(3) \ , \ 0 \ , \ -w(1)]^T}{\sqrt{(w(3))^2 + (-w(1))^2}} \tag{4}$$

The vector $\mathbf{v}$ is perpendicular to the plane formed by the vectors $\mathbf{u}$ and $\mathbf{w}$

$$\mathbf{v} = \mathbf{w} \wedge \mathbf{u} \tag{5}$$

The rotation matrix of the matrix ${}^t_{base}T$ can thus be obtained. The constraint of the input grid makes the needle less flexible as it applies a supporting force, so we can assume that the needle can be considered as a rigid tube. Thus, we can relate the coordinates of the needle tip to the point M_f of the CoBra guide robot, knowing the dimensions of the needle.

$$\begin{aligned} {}^t_bT &= {}^{Mf}_bT\,{}^{Mm}_{Mf}T\,{}^t_{Mm}T \\ {}^{Mf}_bT &= {}^t_bT({}^t_{Mm}T)^{-1}\left({}^{Mm}_{Mf}T\right)^{-1} \end{aligned} \tag{6}$$

The value of L_g can therefore be deduced

$$L_g = \frac{g + g_0 - {}^{Mf}_{b}T(3,4))}{{}^{Mf}_{b}T(3,3)} \tag{7}$$

Where g and g_0 are the geometric parameters of the robot. Given the value of L_g, it is therefore possible to obtain the transformation matrix

$${}^{Mr}_{b}T = {}^{Mf}_{b}T\ {}^{Mr}_{Mf}T(L_g) \tag{8}$$

From the transformation matrix ${}^{Mr}_{b}T$ and ${}^{Mf}_{b}T$ represent the transformation matrix of the points M_r and M_f, respectively, relative to the base frame of the robot, the values of the joint positions L_{f1}, L_{f2}, L_{r1} and L_{r2} can be deduced .

$$\begin{array}{l} L_{f1} = {}^{Mf}_{b}T(1,4) - d_1.cos(\alpha_1) - i_1; \\ L_{f2} = L_{f1} + c_1.cos(\alpha_1) + e_1.cos(\beta_1) \end{array} \tag{9}$$

Where :

$\alpha_1 = \arcsin\left(\frac{{}^{Mf}_{b}T(2,4) - (a_1 + b_1/2 + f_1)}{d_1}\right)$ and

$\beta_1 = \left(\frac{a_1 + b_1 + c_1.\sin(\alpha_1)}{e_1}\right)$

The same applies to the rear part of the robot :

$$\begin{array}{l} L_{r1} = {}^{Mr}_{b}T(1,4) - d_2.cos(\alpha_2) - i_2; \\ L_{r2} = L_{r1} + c_2.cos(\alpha_2) + e_2.cos(\beta_2) \end{array} \tag{10}$$

Where :

$\alpha_2 = \arcsin\left(\frac{{}^{Mr}_{b}T(2,4) - (a_2 + b_2/2 + f_2)}{d_2}\right)$ and

$\beta_2 = \left(\frac{a_2 + b_2 + c_2.\sin(\alpha)}{e_2}\right)$

a_1, a_2,b_1,b_2,c_1, c_2,e_1,e_2,f_1,f_2,i_1 and i_2 represent the geometric parameters of the robot, as illustrated in Fig. 4.

IV. Adaptative Control System of Needle Path Planning

In this study we will focus on the adaptive control system part in Fig. 5.(a) for needle path planning represents a subsystem within a larger therapeutic framework. This system is responsible for the real-time adjustment of needle trajectories during brachytherapy, ensuring high precision in targeting and treatment delivery. The aspects related to the instrumentation Fig. 5.(d), modelling Fig. 5.(b), and control Fig. 5.(c) of the Cobra robot have been the subject of further developments and previous studies [1], [5], [6].

This subsystem comprises two main components:

- **AI-based Prediction Model:** This model analyzes real-time organ motion from MRI data (see Fig. 1) to forecast the prostate's movement, allowing for proactive adjustments to the needle path.
- **Adaptive Optimization:** Using the predictive model's output, this module calculates optimal needle insertion points, ensuring efficient cancerous area coverage while minimizing tissue damage and the number of insertions.

This section involves the adaptive control system's role within the complex network of processes and technologies involved in it, highlighting its critical function in enhancing treatment outcomes.

A. Study Hypotheses

This study is guided by key hypotheses for developing the predictive model and optimization framework:

1) **Prostate Motion:** The prostate is assumed to undergo only translational and rotational movements during brachytherapy, focusing on six degrees of freedom (translation and rotation along x, y, z axes) without considering deformation.
2) **Needle Interaction:** The needle's influence on prostate motion is assumed minimal:

$$\Delta p \approx \mathbf{0}, \quad \Delta\theta \approx \mathbf{0} \tag{11}$$

where Δp is the change in the prostate's position vector and $\Delta\theta$ is the change in orientation vector due to needle insertion.

These hypotheses simplify the problem space, aiding the design of the adaptive optimization algorithm and AI-based predictive model to enhance brachytherapy precision and efficacy.

B. Prostate Motion AI-based Prediction Model

In prostate cancer brachytherapy, the Prostate Motion AI-based Prediction Model focuses on translational movements, ignoring deformations. Advanced time series forecasting models are essential for accurate organ movement tracking during procedures. Convolutional Neural Networks (CNNs) detect spatial patterns [7], [8], while Long Short-Term Memory (LSTM) networks capture extended sequences [9], [10]. Graph-based models manage topological data [11]–[13], and hypergraph models handle complex relationships, useful in various domains [14].

Dynamic MRI techniques enable real-time motion tracking, addressing motion artifacts [15]–[18]. Deep learning models enhance motion prediction in healthcare, promising better diagnostic accuracy [19], [20]. The model uses real motion data from 162 patients over five sessions [21] to capture the stochastic nature of prostate movement during therapy.

The chosen architecture is a CNN-LSTM model (Fig. 6), combining CNNs for spatial feature extraction from MRI sequences and LSTMs for temporal pattern recognition. CNNs identify spatial patterns, while LSTMs capture long-term dependencies in sequential data [22]. The spatial-temporal data, X_t, represents the 3D position and orientation of the prostate's center of gravity at time t. Accurate tracking is crucial in precision medicine, especially in brachytherapy, to optimize radiation dose delivery and minimize damage to healthy tissues [23]. Recent advancements in deep learning improve real-time image-guided therapies for prostate cancer, enhancing treatment outcomes [24].

The predictive model is formally expressed as:

$$P_{t+1} = \text{CNN-LSTM}(P_t, P_{t-1}, \ldots, P_{t-n}) \tag{12}$$

The training process involves the minimization of the Mean Squared Error (MSE) between the predicted and actual positions and orientations of the prostate's center of gravity:

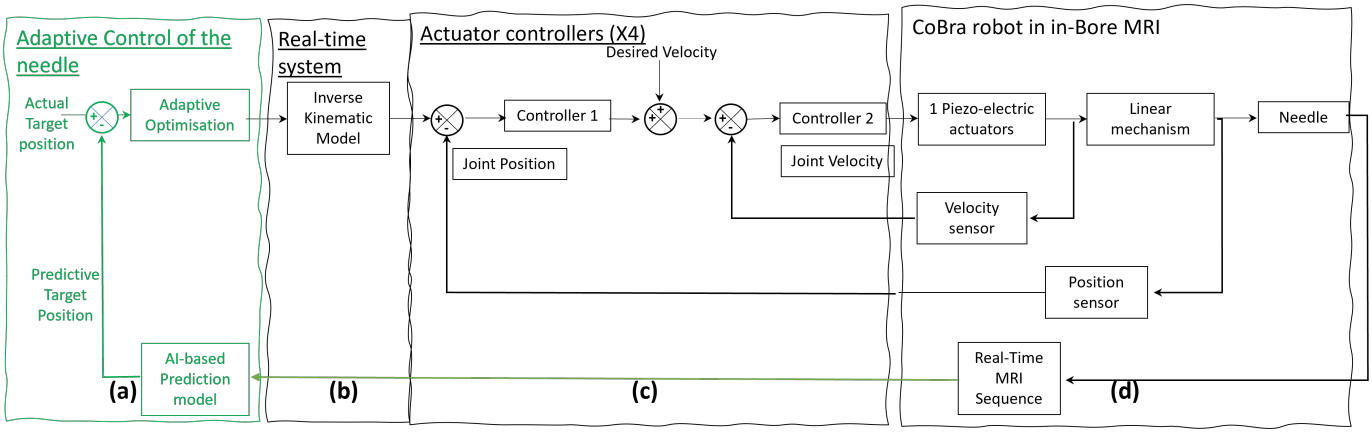

Fig. 5. Block diagram of the autonomous control of needle insertion by the CoBra robot, featuring an AI-based prediction model for adaptive target tracking, accommodating anatomical changes in the prostate. The control architecture consists of four main parts: adaptive needle control, NI-CompactRIO real-time system, actuator controllers, and MRI-based CoBra robot.

Fig. 6. CNN-LSTM Motion Prediction Model

$$\min \text{MSE} = \frac{1}{N}\sum_{i=1}^{N}(X_{t+1}^{(i)} - \hat{X}_{t+1}^{(i)})^2 \tag{13}$$

where $\hat{X}_{t+1}^{(i)}$ represents the predicted position and orientation, and $X_{t+1}^{(i)}$ represents the true position and orientation at time $t+1$. This optimization criterion ensures that the model provides the most accurate real-time predictions of prostate motion, which are critical for adjusting the needle trajectory during the brachytherapy procedure, thereby enhancing the precision and safety of the treatment.

C. Path Planning Adaptive Optimisation

Conventional biopsy and brachytherapy methods use a grid system for parallel needle insertions, requiring multiple insertions to cover the prostate. This method doesn't account for prostate movement. The MPEP approach [25] reduces insertions while optimizing tumor targeting. The CoBra template grid (CTG) guides needle paths at various angles, adapting to prostate motion for better targeting.

This research extends MPEP by incorporating dynamic prostate positioning to improve adaptive optimization. The goal is to reduce needle insertions while maintaining precise targeting, considering prostate movement (Fig. 7). Mathematically, let I_f be a set of N target points P_f, and I_e a set of N_e entry points P_e. A treatment requires N paths P_eP_f such that $P_f \in I_f$ and $P_e \in I_e$, with efficient paths minimizing entry points and robot travel distance.

The adaptive control module, shown in green in Fig. 5, is based on an AI-driven prediction model that uses real-time MRI data. This model predicts the future position of the prostate P_{future} based on current and past observed positions $P_{current}$ and P_{past}:

$$P_f^{t+1} = f(P_f^{t-k,\ldots,t}) \tag{14}$$

Given a set of target points $\{P_{f_1}, P_{f_2}, ..., P_{f_n}\}$ and a set of entry points $\{P_{e_1}, P_{e_2}, ..., P_{e_m}\}$, the cost function is defined as:

$$\min C = \alpha R + \beta D + \lambda E \tag{15}$$

where:

- R represents the total distance between each entry point and its corresponding target point. For each path i from an entry point P_{e_i} to a target point P_{f_i}, the distance d_i is calculated. The total distance is L:

$$R = \sum_{i=1}^{N} d(P_{e_i}, P_{f_i}) \tag{16}$$

- D is the sum of deviations from the predicted target positions. For a predicted target position $\hat{P}_{f_i}$ and the actual target position P_{f_i}, the deviation δ_i is the difference between them. D is the total of all such deviations:

$$D = \sum_{i=1}^{N} ||\hat{P}_{f_i} - P_{f_i}|| \tag{17}$$

- E is the count of entry points used in the procedure. If an entry point P_{e_j} is utilized for any target point P_{f_i}, it is counted:

$$E = |\{P_{e_j} : \exists P_{f_i} \text{ such that } P_{e_j} \text{ is used to reach } P_{f_i}\}| \tag{18}$$

Algorithm 1 shows the steps for the adaptive optimisation procedure

Algorithm 1 Dynamic Entry Point Selection

procedure ENTRYPOINTSELECTION(V, E, reachability_predictor)
  Create initial mapping of $P_e \rightarrow P_f$
  Select first P_{e_i} based on initial mapping
  Place seed at selected P_{e_i}
  Get updated reachability predictions from $reachability\_predictor$ for remaining $P_e - \{P_{e_i}\}$ given current placements
  Update mapping of $P_e \rightarrow \hat{P}_f$
  $P_f = P_f - \{P_{f_i} | P_{f_i}$ is reachable by $P_{e_i}\}$
  while $P_f \neq \phi$ **do**
    Select next best P_{e_i} using updated mapping
    Place seed at selected P_{e_i}
    Get updated predictions for remaining P_f
    Update mapping of $P_e \rightarrow \hat{P}_f$
    $P_f = P_f - \{P_{f_i} | P_{f_i}$ is reachable by $P_{e_i}\}$
  end while
end procedure

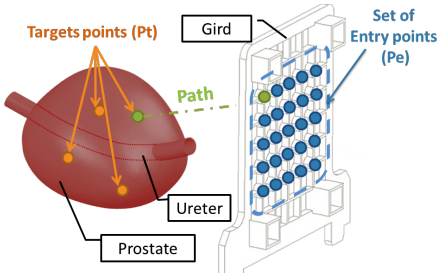

Fig. 7. Optimization Problem: Blue points indicate the grid's entry points on the perineal skin, while orange points denote target tumors in the prostate. Each needle path (green) is defined by a target point and an entry point.

V. EXPERIMENTAL RESULTS

A. Dataset and Hardware Environment

a) Dataset: The dataset for training the Prostate Motion AI-based Prediction Model comprises motion data collected from 162 patients undergoing radiotherapy. Each patient's prostate motion was recorded over five (or six) sessions, resulting in a comprehensive dataset that captures a wide array of movement patterns. The recorded data specifically includes the 3D position and orientation of the prostate's center of gravity (See Fig. 8, providing the spatial-temporal sequences necessary for the predictive modeling.

b) Hardware Environment: The training and development of the CNN-LSTM model were conducted on a personal laptop. The hardware environmentis equipped with an AMD Ryzen 7 7745HX processor, 32GB of RAM, and an NVIDIA RTX 4070 graphics card. The NVIDIA RTX 4070 is outfitted with tensor cores optimized for AI tasks and supports CUDA program workloads.

This robust hardware setup ensures that the CNN-LSTM model can be trained efficiently, with the GPU acceleration being particularly critical for handling the computationally intensive tasks involved in training deep learning models.

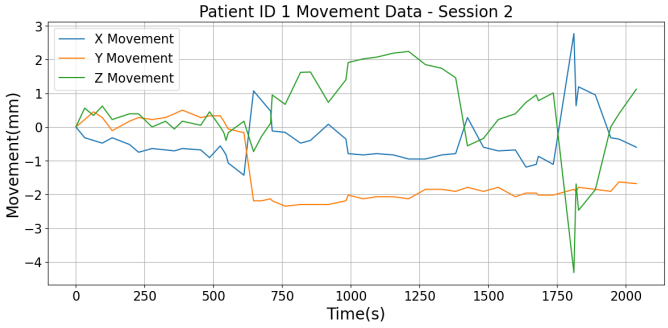

Fig. 8. Patient 1 X,Y,Z Movements during Session 2

B. Training and Validation Performance

The model's performance was evaluated using Mean Squared Error (MSE) as the loss function, quantifying the average squared difference between estimated and actual values. During training, the model achieved a best MSE of approximately $1.44\,\text{mm}^2$, indicating high accuracy in predicting the prostate's center of gravity.

Fig. 9. Training and Validation MSE of the CNN-LSTM Model

Fig. 9 shows the model's learning curve, with the x-axis representing epochs and the y-axis representing MSE. The plot displays decreasing MSE trends for both training and validation datasets as epochs increase.

C. Adaptive Optimisation Result

The model's performance, evaluated using Mean Squared Error (MSE), achieved a best MSE of approximately $1.44\,\text{mm}^2$, indicating high accuracy in predicting the prostate's center of gravity.

Fig. 9 shows the learning curve, with MSE decreasing as epochs increase for both training and validation datasets.

The adaptive optimization algorithm was compared to the static approach across ten procedures (Fig. 10). The dynamic method reduced the average number of needles from 7.8 to 7.3 and increased coverage from 80.28% to 96.4%, demonstrating a 12.72% improvement.

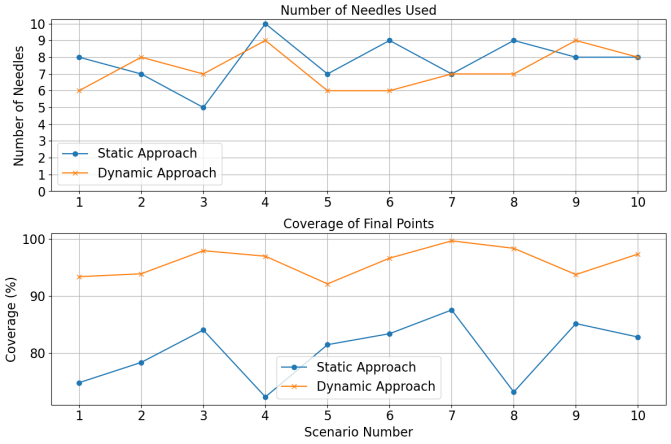

Fig. 10. Performance Comparison Between Static and Adaptive Approaches

In summary, the adaptive optimization approach is more efficient and effective than the static method, ensuring optimal needle usage and excellent coverage for brachytherapy. Future work will expand this approach to other procedures and refine the algorithm for better decision-making.

VI. Conclusion and Future Work

This work presents a dynamic optimisation approach for needle path planning in prostate brachytherapy, leveraging real-time MRI data and advanced predictive modelling. The adaptive method significantly reduces needle usage and enhances procedural efficiency, outperforming traditional static methods. Despite the computational demand, the integration of AI prediction algorithms with robotic kinematics allows for real-time adjustments, improving surgical precision and resource utilisation.

The model's assumptions, such as focusing only on translational and rotational movements and neglecting the needle's impact on prostate movement, need further evaluation. Future work should refine the optimization algorithm, expand clinical applications, and incorporate comprehensive predictive models to enhance treatment effectiveness. This approach advances brachytherapy and other precision-critical medical procedures.

Acknowledgment

This work has been realized with the support of EU funds in the framework of CoBra (2S04-022) project from the 2 Seas Interreg Programme.

References

[1] A. Belarouci *et al.*, "Cooperative brachytherapy robotic concept for localized cancer treatment under real-time mri," *IEEE Transactions on Medical Robotics and Bionics*, 2022.

[2] A. Jain *et al.*, "Intra-operative 3d guidance and edema detection in prostate brachytherapy using a non-isocentric c-arm," *Medical image analysis*, vol. 16, no. 3, pp. 731–743, 2012.

[3] P. Moreira *et al.*, "The miriam robot: A novel robotic system for mr-guided needle insertion in the prostate," *Journal of medical robotics research*, vol. 2, no. 04, p. 1750006, 2017.

[4] A. Belarouci, S. S. Dhaliwal, M. Sanz-Lopez, F. Verbrugghe, O. Lakhal, T. Chettibi, and R. Merzouki, "Cooperative brachytherapy robotic concept for localized cancer treatment under real-time mri," *IEEE Transactions on Medical Robotics and Bionics*, vol. 4, no. 3, 2022.

[5] S. S. Dhaliwal, T. Chettibi, A. Belarouci, G. Dherbomez, V. Coelen, and R. Merzouki, "Cooperative brachytherapy for prostate cancer under mri guidance," in *2019 Fifth International Conference on Advances in Biomedical Engineering (ICABME)*. IEEE, 2019, pp. 1–4.

[6] S. S. Dhaliwal, S. Wilby, S. Firouzy, K. B. Boni, M. de Vries, S. E. Navarro, A. Belarouci, V. Coelen, O. Lakhal, D. Pasquier *et al.*, "Cobra robot for localized cancer treatment and diagnosis under real-time mri," in *AUTOMED 2021-Interdisciplinary Symposium Automation in Medical Engineering*, 2021.

[7] S. Bai, J. Z. Kolter, and V. Koltun, "An empirical evaluation of generic convolutional and recurrent networks for sequence modeling," *arXiv preprint arXiv:1803.01271*, 2018.

[8] M. Ismail and A. Sengur, "Deep learning-based time series forecasting: An experimental evaluation," *Neural Computing and Applications*, 2021.

[9] A. Chauhan and L. Vig, "Anomaly detection in ecg time signals via deep long short-term memory networks," in *2015 IEEE International Conference on Data Science and Advanced Analytics (DSAA)*, 2015.

[10] X. Yang, S. Zhang, X. Zhang, D. Wu, and J. Su, *Machine Learning and Deep Learning Based Time Series Prediction and Forecasting of Ten Nations' COVID-19 Pandemic*. Springer, 2023.

[11] H. Xiao, Y. Huang, Z. Pan, W. Li, Y. Hu, and G. Lin, "Multi-task time series forecasting based on graph neural networks," *MDPI*, 2023.

[12] Z. Wang, F. Zhou, G. Trajcevski, K. Zhang, and T. Zhong, "Learning dynamic temporal relations with continuous graph for multivariate time series forecasting," in *AAAI*, 2023.

[13] L. Liao, Z. Hu, C. Y. Hsu, and J. Su, "Fourier graph convolution network for time series prediction," *MDPI*, 2023.

[14] T. T. Huynh, M. H. Nguyen, T. Nguyen, P. L. Nguyen, M. Weidlich, Q. V. H. Nguyen, and K. Aberer, "Efficient integration of multi-order dynamics and internal dynamics in stock movement prediction," *ACM*, 2022.

[15] S. Purushotham, C. Meng, Z. Che, and Y. Liu, "Benchmark of deep learning models on large healthcare mimic datasets," *arXiv preprint arXiv:1710.08531*, 2019.

[16] L. J. Frohwein, F. Büther, and K. P. Schäfers, "Estimation of physiological motion using highly accelerated continuous 2d mri," *arXiv preprint arXiv:1905.08176*, 2019.

[17] M. Bengs, J. Sprenger, S. Gerlach, M. Neidhardt, and A. Schlaefer, "Real-time motion analysis with 4d deep learning for ultrasound-guided radiotherapy," *IEEE Transactions on Biomedical Engineering*, 2023.

[18] D. Li, W. Zhong, K. M. Deh, T. D. Nguyen, M. R. Prince, Y. Wang, and P. Spincemaille, "Discontinuity preserving liver mr registration with three-dimensional active contour motion segmentation," *IEEE Transactions on Biomedical Engineering*, vol. 66, no. 7, pp. 1884–1897, 2019.

[19] M. A. Morid, O. R. L. Sheng, and J. Dunbar, "Time series prediction using deep learning methods in healthcare," *arXiv preprint arXiv:2108.13461*, 2021.

[20] J. Krebs, T. Mansi, N. Ayache, and H. Delingette, "Probabilistic motion modeling from medical image sequences: Application to cardiac cine-mri," *arXiv preprint arXiv:1907.13524*, 2019.

[21] A. Taillez, A.-M. Bimbai, T. Lacornerie, M.-C. Le Deley, E. F. Lartigau, and D. Pasquier, "Studies of intra-fraction prostate motion during stereotactic irradiation in first irradiation and re-irradiation," *Frontiers in Oncology*, vol. 11, 2021.

[22] M. Keerthana, G. V. R. Reddy, and M. K. B. Maruthiram, "Landmark tracking in liver us images using cascade convolutional neural networks with long short-term memory," *International Journal for Research in Applied Science and Engineering Technology (IJRASET)*, 2023.

[23] Y. Zhang, X. Dai, Z. Tian, Y. Lei, J. Wynne, P. Patel, Y. Chen, T. Liu, and X. Yang, "Landmark tracking in liver us images using cascade convolutional neural networks with long short-term memory," *Physiological Measurement*, vol. 43, no. 9, p. 095003, 2022.

[24] D. Chrystall, A. Mylonas, E. Hewson, J. Martin, P. Keall, J. Booth, and D. Nguyen, "Deep learning enables mv-based real-time image guided radiation therapy for prostate cancer patients," *Physics in Medicine Biology*, 2023.

[25] O. Lakhal, T. Chettibi, A. Belarouci, K. Youcef-Toumi, and R. Merzouki, "Optimisation of path planning for minimally invasive interventions on prostate using mr-robot: Application to on-live pets," *IFAC-PapersOnLine*, 2023, 22nd IFAC World Congress.